Sensors and Materials, Vol. 33, No. 5 (2021) 1739–1747
MYU Tokyo

S & M 2568

Annealing Temperature Dependence of Upconversion Phosphor of TiO_2-ZnO Doped with Yb^{3+} and Tm^{3+}

Toshihiro Nonaka,* Takahiko Ban, and Shin-Ichi Yamamoto

Course of Electronics, Information and Communication Engineering, Faculty of Advanced Science and Technology, Ryukoku University, 1-5 Yokotani, Seta Oe-cho, Otsu, Shiga 520-2194, Japan

(Received March 15, 2021; accepted April 30, 2021)

Keywords: upconversion, TiO_2-ZnO, Yb^{3+}, Tm^{3+}, metal-organic decomposition

In this paper, we report on the annealing temperature dependence of the upconversion (UC) phosphor of TiO_2-ZnO doped with Yb^{3+} and Tm^{3+}. We prepared samples using metal-organic decomposition (MOD) solutions and Tm_2O_3 powder, which were analyzed in terms of their photoluminescence (PL) spectra and crystal structures. The PL spectra showed a blue UC phosphor band at a wavelength of 476 nm. The emission intensity was greatest after annealing at 850 °C. By analyzing the crystal structures using an X-ray diffractometer (XRD), it was found that there was a large amount of $RE_2Ti_2O_7$ in the samples annealed at 900 °C and above.

1. Introduction

Upconversion (UC) luminescent materials have been attracting significant attention recently owing to their potential use in a variety of fields.[1–4] When excited by light of a particular wavelength, ordinary luminescent materials discharge light with a wavelength longer than that of the incident light. This difference in energy is referred to as the Stokes shift and is attributed to the thermal energy generated within the material. On the other hand, UC is a phenomenon in which light with a wavelength shorter than the excitation wavelength is emitted; this phenomenon is also referred to as anti-Stokes emission. Rare-earth ions with long excited-state lifetimes are generally used as luminescent centers for UC. Infrared or near-infrared light is used as the excitation light for generating the visible light with UC.

Studies are currently being conducted on halides and metal oxides as host materials for UC. Halides have been intensively studied, particularly fluorides.[5,6] However, the disadvantage of using these materials is their susceptibility to damage by exposure to air as they are affected by moisture. For this reason, attempts have been made to disperse crystal particles in glass or to crystallize them in glass. On the other hand, materials with good luminous efficiency are being sought among metal oxide host materials due to their high stability upon air exposure. However, their luminous efficiency is inferior to that of fluorides.

The physico-chemical properties of materials based on titanium dioxides have been reported in various studies.[7–11] The fabrication and application of Zn_2TiO_4 are attracting attention owing

*Corresponding author: e-maill: t-nonaka@toyota-ct.ac.jp
https://doi.org/10.18494/SAM.2021.3364

ISSN 0914-4935

to its inverse spinel structure and high thermal stability.[12] In particular, oxides composed of ZnO and TiO_2 are being studied for applications such as gas sensors,[10] photocatalysts,[13] chemical sorbing,[12] and downconversion.[14] Luitel *et al.* fabricated a UC phosphor by using ZnO-TiO_2 and reported its superior emission intensity to that of ZnO-TiO_2.[15]

Focusing on the potential of ZnO-TiO_2 as a host material for UC, we fabricated a UC phosphor by doping ZnO-TiO_2 with Yb^{3+} and Er^{3+}, then evaluated its characteristics.[16] A drawback of this phosphor was that multiple emission spectra appeared when ZnO-TiO_2 was doped with Yb^{3+} and Er^{3+}, implying that this material cannot be used as one of the three primary light colors. Thus, the UC phosphor was prepared by doping ZnO-TiO_2 with Yb^{3+} and Tm^{3+}, then its characteristics were evaluated. Strong emission of blue light could potentially be achieved around a wavelength of 480 nm by doping ZnO-TiO_2 with Yb^{3+} and Tm^{3+}.[17,18]

In 2018, Kobwittaya *et al.* reported a phosphor in which ZnO-TiO_2 was doped with Yb^{3+} and Tm^{3+} by a powder–solution mixing method.[19] However, they did not realize the blue color near 480 nm. In contrast, this paper is the world's first report of blue light emission realized with a ZnO-TiO_2 host material.

UC phosphors are typically fabricated by sputtering,[20] sintering,[21] or the sol-gel method.[22] In this study, we fabricated a UC phosphor by using metal-organic decomposition (MOD) to simplify the fabrication process.[23–25]

2. Materials and Methods

2.1 Fabrication of UC

We fabricated a UC phosphor using only MOD solutions by following the method shown in Fig. 1(a). The MOD solutions (TiO_2, ZnO, Yb_2O_3, and $TmO_{1.5}$), supplied by Kojundo Chemical

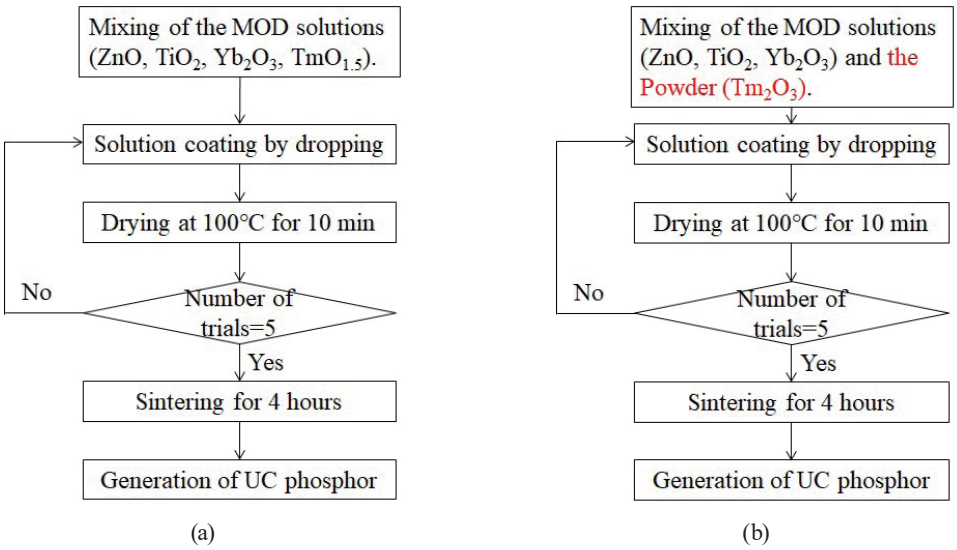

Fig. 1. (Color online) Flowchart of UC phosphor synthesis process: (a) UC phosphor fabricated using only MOD solutions (b) and UC phosphor fabricated using MOD solutions with Tm_2O_3 powder.

Laboratory, were used as the sources of Ti, Zn, Yb, and Tm. The MOD solutions were mixed so that the molar ratio of the elements was Ti:Zn:Yb:Tm = 1:1:0.06:0.04. 0.05 ml of the mixed MOD solution was applied to a Si substrate (100), which was then dried at 100 °C for 10 min. This operation was repeated five times. Then, the sample was heated for 4 h at 850 °C.

We also fabricated UC phosphor specimens using MOD solutions and Tm_2O_3 powder by following the method shown in Fig. 1(b). The MOD solutions (TiO_2, ZnO, and Yb_2O_3), supplied by Kojundo, were used as the sources of Ti, Zn, and Yb. Tm_2O_3 powder, supplied by Kojundo, was used as the source of Tm. The MOD solutions and Tm_2O_3 powder were mixed so that the molar ratio of the elements was Ti:Zn:Yb:Tm = 1:1:0.06:0.04. 0.05 ml of the mixed MOD solution was applied to a Si substrate (100), which was then dried at 100 °C for 10 min. This operation was repeated five times. Then, the sample was heated for 4 h at 850 °C.

The photoluminescence (PL) spectra were measured using a near-infrared laser (200 mW) with a wavelength of 980 nm as the excitation light. The sample was irradiated with the near-infrared laser at an angle of 45°, and the generated light was observed from directly above using an Ocean Optics spectrometer.[16] The spectroscopic measurement range was from 350 to 1050 nm. A calibration was performed by obtaining the dark-line spectrum before the measurement.

2.2 Annealing temperature dependence of UC phosphor fabricated using MOD solutions and Tm_2O_3 powder

We fabricated UC phosphor specimens using MOD solutions and Tm_2O_3 powder by following the method shown in Fig. 1(b). The MOD solutions (TiO_2, ZnO, and Yb_2O_3), supplied by Kojundo, were used as the sources of Ti, Zn, and Yb. Tm_2O_3 powder, supplied by Kojundo, was used as the source of Tm. The MOD solutions and Tm_2O_3 powder were mixed so that the molar ratio of the elements was Ti:Zn:Yb:Tm = 1:1:0.06:0.04. 0.05 ml of the mixed MOD solution was applied to a Si substrate (100), which was then dried at 100 °C for 10 min. This operation was repeated five times. Then, the sample was heated for 4 h at a temperature of 700, 750, 800, 850, 900, 950, 1000, or 1050 °C. PL spectra of the samples were obtained using a PL spectrometer similarly to in Sect. 2.1, and compounds were identified using an X-ray diffractometer (XRD).

3. Results and Discussion

3.1 Dependence of fabrication process on structural and optical properties

The PL spectrum of the UC phosphor fabricated using only MOD solutions is shown in Fig. 2. From the spectrum, it was clarified that the UC phosphor could not be produced only using the MOD solutions. For comparison, the PL spectrum of the sample fabricated using Tm_2O_3 powder that was annealed at 850 °C is also shown. Peaks were observed at 476 nm ($^1G_4 \rightarrow {}^3H_6$) and 649 nm ($^1G_4 \rightarrow {}^3F_4$).

XRD pattern of the UC phosphor fabricated using only MOD solutions is shown in Fig. 3. For comparison, the XRD pattern of the sample fabricated using Tm_2O_3 powder that was annealed at 850 °C is also shown. The horizontal axis of Fig. 3(a) shows the range of $2\theta = 20–60°$. Standard

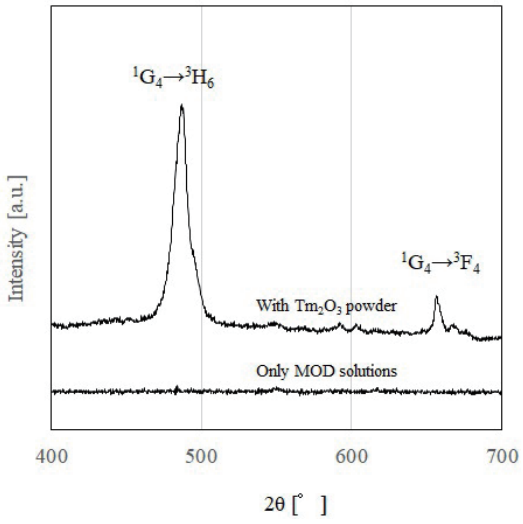

Fig. 2. PL spectra of UC phosphor fabricated using only MOD solutions and UC phosphor fabricated using MOD solutions and Tm_2O_3 powder.

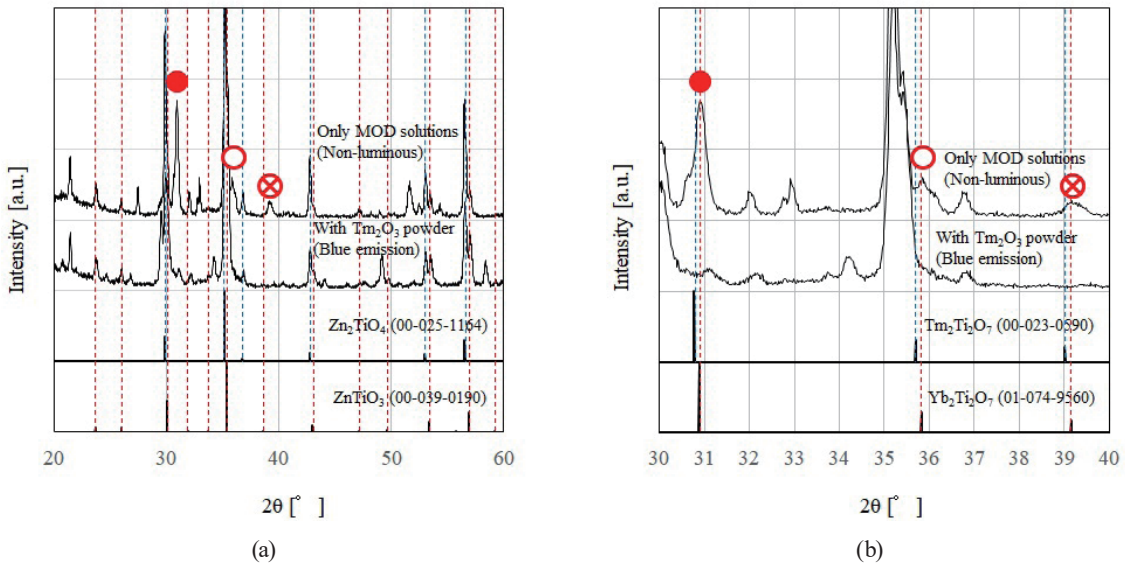

Fig. 3. (Color online) XRD patterns of UC phosphor fabricated using only MOD solutions and UC phosphor fabricated using MOD solutions and Tm_2O_3 powder: (a) $2\theta = 20–60°$ and (b) $2\theta = 30–40°$.

patterns of the Powder Diffraction File (PDF) of Zn_2TiO_4 (00-025-1164) and $ZnTiO_3$ (00-039-0190) are shown at the bottom of Fig. 3(a). From the results, it can be seen that the samples are mostly composed of Zn_2TiO_4 or $ZnTiO_3$. Because the Zn and Ti contents are large compared with those of the rare-earth elements (Yb, Tm), it is considered that Zn_2TiO_4 or $ZnTiO_3$ exists in the two samples.

The horizontal axis of Fig. 3(b) shows the range of 2θ = 30–40°, and the PDF patterns of $Tm_2Ti_2O_7$ (00-023-0590) and $Yb_2Ti_2O_7$ (01-074-9560) are included at the bottom of Fig. 3(b). The peak positions of $Tm_2Ti_2O_7$ and $Yb_2Ti_2O_7$ are close to each other, making it difficult to identify whether the measured peaks are $Tm_2Ti_2O_7$ or $Yb_2Ti_2O_7$. Therefore, in this paper, $RE_2Ti_2O_7$ is used as a generic term for $Tm_2Ti_2O_7$ and $Yb_2Ti_2O_7$. From Fig. 3(b), it can be seen that $RE_2Ti_2O_7$ is crystallized in the sample fabricated using only MOD solutions. The peak at 30.9° in Fig. 3(b) is the main peak of $RE_2Ti_2O_7$ (2 2 2). It is considered that in the sample fabricated using only MOD solutions, the constituent elements are efficiently diffused and $RE_2Ti_2O_7$ is crystallized at 850 °C. On the other hand, for the sample fabricated also using Tm_2O_3 powder, it is considered that the Tm element was not efficiently diffused because Tm_2O_3 powder was used.

3.2 Annealing temperature dependence of UC phosphor fabricated using MOD solutions and Tm_2O_3 powder

The PL spectra of the UC phosphor fabricated also using Tm_2O_3 are shown in Fig. 4. The emission intensity increases with the annealing temperature from 700 to 850 °C. An emission peak is observed at 476 nm (blue light, corresponding to $^1G_4 \rightarrow {}^3H_6$), and another smaller peak is observed at 649 nm (corresponding to $^1G_4 \rightarrow {}^3F_4$). The emission intensity is clearly reduced when the annealing temperature is further increased to 900 °C. At 950 °C and above, almost no emission is observed.

The XRD patterns of the TiO_2-ZnO UC phosphor doped with Yb^{3+} and Tm^{3+} and annealed at 700–1050 °C are shown in Fig. 5. The horizontal axis of Fig. 5(a) shows the range of 2θ = 20–60°. Standard patterns of the PDF of Zn_2TiO_4 (00-025-1164) and $ZnTiO_3$ (00-039-0190) are

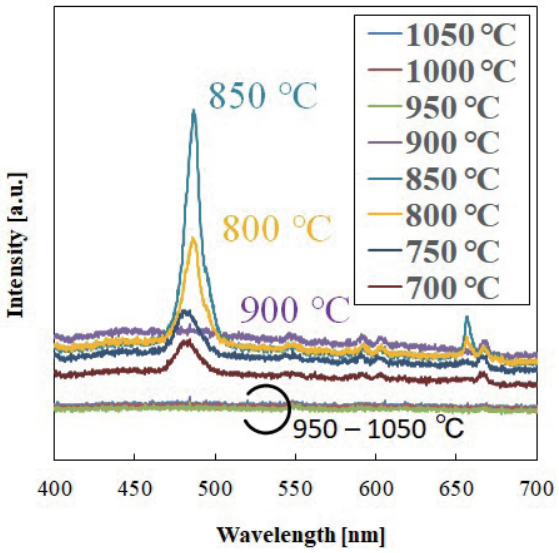

Fig. 4. (Color online) PL spectra of TiO_2-ZnO doped with Yb^{3+} and Tm^{3+} and annealed at 700–1050 °C.

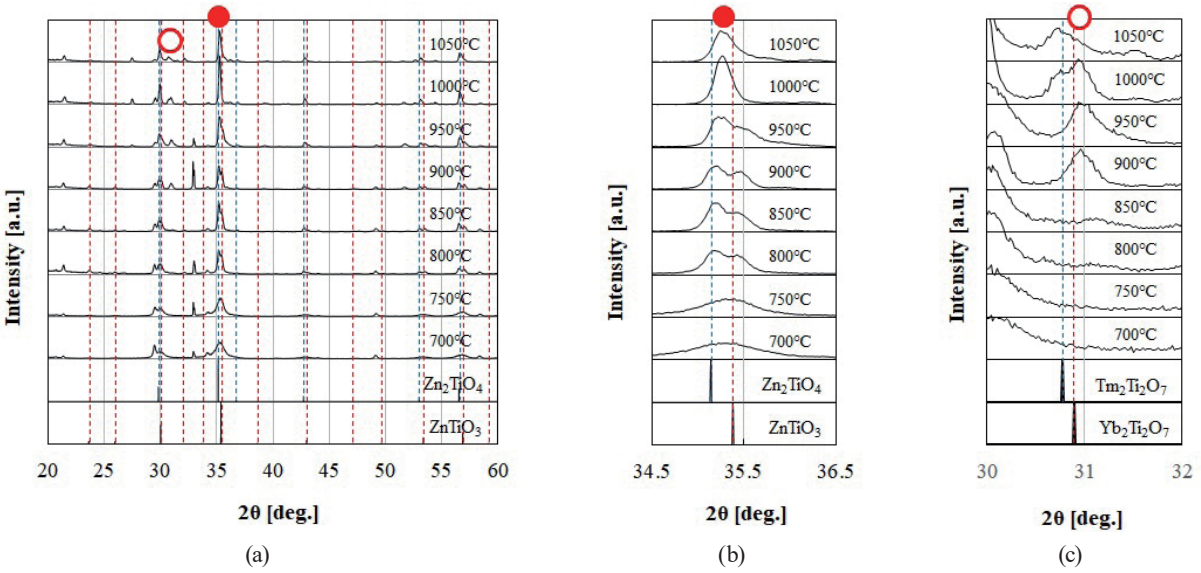

Fig. 5. (Color online) XRD patterns of TiO_2-ZnO UC phosphor doped with Yb^{3+} and Tm^{3+} and annealed at 700–1050 °C: (a) 2θ = 20–60°, (b) 2θ = 34.5–36.5°, and (c) 2θ = 30–32°.

shown at the bottom of Fig. 5(a). The horizontal axis of Fig. 5(b) shows the range of 2θ = 34.5–36.5° with PDF patterns of Zn_2TiO_4 (00-025-1164) and $ZnTiO_3$ (00-039-0190) at the bottom. The horizontal axis of Fig. 5(c) shows the range of 2θ = 30–32° with PDF patterns of $Tm_2Ti_2O_7$ (00-023-0590) and $Yb_2Ti_2O_7$ (01-074-9560) at the bottom.

From the results in Fig. 5(a), it can be seen that the samples are mainly composed of Zn_2TiO_4 or $ZnTiO_3$. Because the Zn and Ti contents are large compared with those of the rare-earth elements (Yb, Tm), it is considered that Zn_2TiO_4 or $ZnTiO_3$ exists in the samples. Figure 5(b) shows the major peaks of Zn_2TiO_4 and $ZnTiO_3$, from which it can be seen that Zn_2TiO_4 and $ZnTiO_3$ coexist in the samples annealed from 700 to 950 °C but Zn_2TiO_4 is contained in the samples annealed at 1000 °C and above. From the results shown in Fig. 4, a decrease in PL intensity occurs at 900 °C and above. In addition, the integrated intensity of Zn_2TiO_4, which is considered to be the host material, has no correlation with the PL spectra. Figure 5(c) shows the major peak of $RE_2Ti_2O_7$ (2 2 2) . It can be seen that the $RE_2Ti_2O_7$ content begins to increase at 900 °C and above. From the PL spectra in Fig. 4, the emission intensity decreased from an annealing temperature of 900 °C. There is an inverse correlation between the PL intensity and the amount of $RE_2Ti_2O_7$ precipitation. Figure 6 shows equilibrium diagrams between TiO_2 and ZnO [Fig. 6(a)],[26] TiO_2 and TmO_3 [Fig. 6(b)],[27] and TiO_2 and Yb_2O_3 [Fig. 6(c)].[28]

In this study, since samples were prepared with a molar ratio of Zn:Ti = 1:1, we focus on intermediate molar contents in Fig. 6(a). The figure shows that $ZnTiO_3$ disappears above 945 °C. According to Fig. 5(b), Zn_2TiO_4 accounts for most of the samples annealed at 950 °C and above, which is consistent with Fig. 6(a).

In this study, TiO_2 is more abundant in the samples than Tm_2O_3 or Yb_2O_3, so we focus on the TiO_2-rich side in Figs. 6(b) and 6(c). There is no phase diagram in the temperature range below

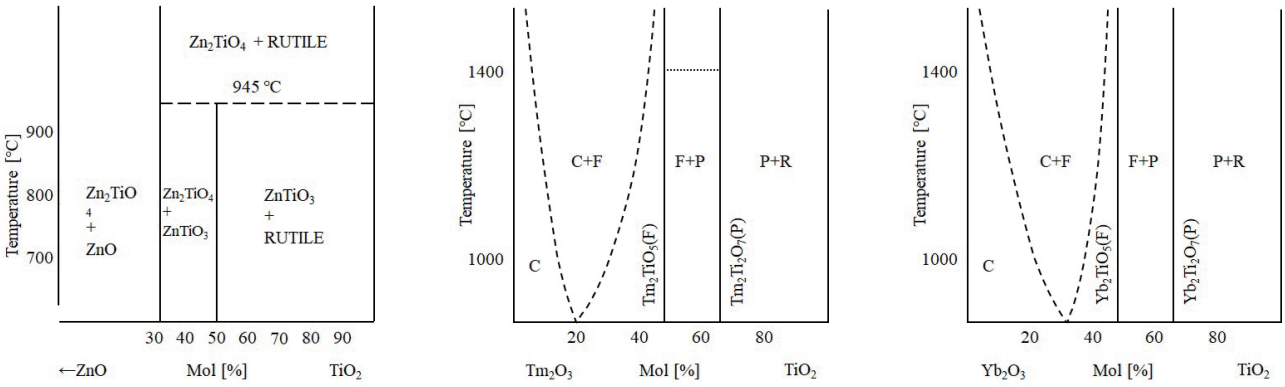

Fig. 6. Equilibrium diagrams: (a) TiO_2 and ZnO[26] (R = TiO_2 [rutile]), (b) TiO_2 and Tm_2O_3[27] (C = cubic solid solution based on Tm_2O_3; F = Tm_2TiO_5 [fluorite structure]; P = $Tm_2Ti_2O_7$ [pyrochlore structure]; R = TiO_2 [rutile]), and (c) TiO_2 and Yb_2O_3[28] (C = cubic solid solution based on Yb_2O_3; F = Yb_2TiO_5 [fluorite structure]; P = $Yb_2Ti_2O_7$ [pyrochlore structure]; R = TiO_2 [rutile]).

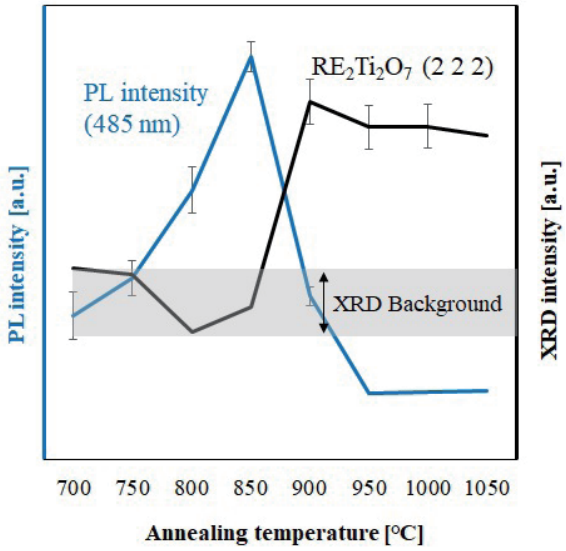

Fig. 7. (Color online) Annealing temperature dependences of $RE_2Ti_2O_7$ (2 2 2) XRD peak intensity and PL emission intensity.

1000 °C. Therefore, Fig. 5(c) is the world's first datum that found the temperature at which $RE_2Ti_2O_7$ appears.

The annealing temperature dependences of the $RE_2Ti_2O_7$ (2 2 2) XRD peak intensity and PL emission intensity are shown in Fig. 7. The horizontal axis shows the annealing temperature and the vertical axis shows the PL emission intensity and XRD intensity. Since the peak of $RE_2Ti_2O_7$ (2 2 2) is not observed at 700, 750, 800, and 850 °C, the plotted values are background values. On the other hand, the PL emission intensity of 485 nm increases from 700 to 850 °C. Therefore, it

is considered that the luminescence intensity is increased because the crystallization of the substance emitting light is promoted, and large amounts of Yb^{3+} and Tm^{3+} are dissolved in the host material. The cause of the decrease in emission intensity from 900 to 1050 °C is thought to be related to the increase in the $RE_2Ti_2O_7$ content, because $RE_2Ti_2O_7$ peaks appear at 900 °C and above and the emission intensity also begins to decrease at 900 °C. In the UC of blue emission, an electron that transitions from $^2F_{7/2}$ to $^2F_{5/2}$ of Yb^{3+} is transferred to the $^1G_4$ band of Tm^{3+}, and when it returns to the ground state of $^3H_6$, an electromagnetic wave of 485 nm is emitted.[18] It is considered that the emission intensity decreases at 900 °C or higher because of the increase in the contents of Yb^{3+} and Tm^{3+}, which do not contribute to the emission intensity, due to the increase in the $RE_2Ti_2O_7$ content. Therefore, when preparing ZnO-TiO_2 UC phosphor doped with Tm^{3+} and Yb^{3+} using MOD solutions and Tm_2O_3 powder, it is necessary to find suitable conditions before increasing the $RE_2Ti_2O_7$ content.

4. Conclusions

A blue phosphor for UC was fabricated using MOD solutions (ZnO, TiO_2, Yb_2O_3) and Tm_2O_3 powder. The MOD solutions and the powder were applied to a Si (1 0 0) substrate, which was then annealed at temperatures ranging from 700 to 1050 °C. A near-infrared laser with an output of 200 mW at the 980 nm wavelength was then used to measure the PL spectra and an XRD was used to analyze the compounds. The PL measurements revealed that the emission intensity increased with increasing annealing temperature from 700 to 850 °C. The emission intensity clearly decreased at annealing temperatures of 900 °C and above. In the XRD patterns, peaks of $RE_2Ti_2O_7$ were detected in the samples annealed at 900 °C and above. The emission intensity decreased at 900 °C or above, and this phenomenon is considered to be related to the increase in the $RE_2Ti_2O_7$ content.

Acknowledgments

This work was supported by the Joint Research Center for Science and Technology of Ryukoku University. This work was also partly supported by the ICOM Foundation, Japan.

References

1 H. Lin, G. Meredith, S. Jiang, X. Peng, T. Luo, N. Peyghambarian, and E. Pun: J. Appl. Phys. **93** (2003) 186.
2 G. Yi and G. Chow: Chem. Mater. **19** (2007) 341.
3 E. Cavalli, L. Esposito, J. Hostasa, and M. Pedroni: J. Eur. Ceram. Soc. **33** (2013) 1425.
4 L. Liang, Y. Yulin, Z. Mi, F. Ruiqing, Q. Lele, W. Xin, Z. Lingyun, Z. Xuesong, and H. Jianglong: J. Solid State Chem. **198** (2013) 459.
5 S. Heer, K. Kompe, H. Gudel, and M. Haase: Adv. Mater. **16** (2004) 2102.
6 F. Wang and X. Liu: J. Am. Chem. Soc. **130** (2008) 5642.
7 K. Babu, D. Singh, and O. Srivastava: Semicond. Sci. Technol. **5** (1990) 364.
8 J. Kristof, J. Liszi, P. Szabo, A. Barbieri, and A. Battisti: J. Appl. Electrochem. **23** (1993) 615.
9 V. Berbenni and A. Marini: J. Mater. Sci. **39** (2004) 5279.
10 B. Zhu, C. Xie, W. Wang, K. Huang, and J. Hu: Mater. Lett. **58** (2004) 624.
11 G. Lakshminarayana, J. Qiu, M. Brik, G. Kumar, and I. Kityk: J. Phys.: Condens. Matter **20** (2008) 375101.
12 H. Kim and Y. Kim: J. Am. Ceram. Soc. **84** (2001) 1081.

13 G. Marci, V. Augugliaro, M. Lopez-Munoz, C. Martin, L. Palmisano, V. Rives, M. Schiavello, R. Tilley, and A. Venezia: J. Phys. Chem. B **105** (2001) 1033.
14 B. Jiao, M. Li, X. Zhang, and X. Wang: Adv. Mater. Res. **652** (2013) 622.
15 H. Luitel, K. Ikeue, R. Okuda, R. Chand, T. Torikai, M. Yada, and T. Watari: Opt. Mater. **36** (2014) 591.
16 T. Nonaka, T. Kanamori, K. Ohyama, and S. Yamamoto: Jpn. J. Appl. Phys. **54** (2015) 03CA02.
17 J. Boyer, L. Cuccia, and J. Capobianco: Nano Lett. **7** (2007) 847.
18 D. Simpton, W. Gibbs, S. Collins, W. Blanc, B. Dussardier, G. Monnom, P. Peterka, and G. Baxter: Opt. Express **16** (2008) 13781.
19 K. Kobwittaya, Y. Oishi, T. Torikai, M. Yada, T. Watari, and H. Luitel: Vacuum **148** (2018) 286.
20 P. Kik and A. Polman: J. Appl. Phys. **93** (2003) 5008.
21 X. Qin, J. Zhang, H. Yang, D. Luo, J. Ma, D. Tang, and S. Wang: Solid State Phenom. **185** (2012) 55.
22 B. Dong, C. Li, and X. Wang: J. Sol–Gel Sci. Technol. **44** (2007) 161.
23 I. Yamaguchi, T. Manabe, T. Kumagai, and S. Mizuta: J. Magn. Soc. Jpn. **24** (2000) 1173.
24 L. Son, T. Tachiki, and T. Uchida: Jpn. J. Appl. Phys. **50** (2011) 025803.
25 D. Gallagher, F. Scanlan, R. Houriet, H. Mathieu, and T. Ring: J. Mater. Res. **8** (1993) 3135.
26 F. Dulin and D. Rase: J. Am. Ceram. Soc. **43** (1960) 125.
27 G. Shamrai, R. Magunov, I. Stasenko, and A. Zhirnova: Russ. J. Inorg. Chem. **35** (1990) 450.
28 G. Shamrai, A. Zagorodnyuk, R. Magunov, and A. Zhirnova: Inorg. Mater. **28** (1992) 1633.